MS-2 | 603

MILITARY TECHNICAL COLLEGE
CAIRO - EGYPT

DEVELOPMENT OF A THEORETICAL MODEL TO PREDICT THE STRESS RUPTURE BEHAVIOUR OF COMPOSITE MATERIALS

M.H.ABD EL LATIF*, H.A.HASSAN**

ABSTRACT

Due to their high strength and microstructural stability at elevated temperatures, composite materials are used for turbine blades production, aerospace industries and other several engineering applications.

In this work, a theoretical model is developed to describe the stress rupture behaviour of fibre reinforced composite materials. The model predicts the time to rupture for a certain rupture stress and temperature. It is based upon the interaction between matrix and fibres. Matrix flows under the applied load and an interfacial shear stress is developed at the fibre/matrix interface. This generates a normal stress on the fibre which contributes to the total load bearing capacity of the composite.

Fibre fracture occurs when the normal stress reaches the fibre fracture stress. This may lead to the sudden failure of the composite if the matrix fails to sustain the applied load and the broken fibres are shorter than the transfer length. Failure of the composite may be delayed by the ability of the matrix to sustain the applied stress and reload broken fibres having lengths longer than the transfer length.

Stress concentration arising from microstructural imperfections may cause premature fibre fracture and reduce the time to rupture. To account for that, a stress concentration factor was introduced in the model. Thermal residual stresses resulting from differential thermal expansion mismatch between fibres and matrix are also considered.

---

* Associate Professor, ** Graduate Student, Dpt. of Production Engineering, Faculty of Engineering, Ain Shams University, Cairo, Egypt.

INTRODUCTION

Composite materials are suitable for aircraft and spacecraft industries due to their high strength to weight ratio, and their microstructural stability at elevated temperatures. Since they are involved in the production of engineering components that are expected to withstand service loads at elevated temperatures, it is important to study and analyse their creep rupture behaviour. Most of research efforts were directed to analyse the monotonic behaviour of composites under monotonic loading at ambient temperatures [2,3,4]. Some efforts developed mathematical relations to describe the composite materials behaviour under applied stresses below the yield stress [3,4], and almost no mathematical analysis of the composite behaviour at elevated temperature was found in the literature.

Ashby, Frost and others derived the following relation [1,5] :

$$\dot{\epsilon} = A_2 . D_{ef} . b . \sigma_z^n / 3kT(\sqrt{3}\mu)^{n-1} \qquad (1)$$

connecting the strain rate of the material ($\dot{\epsilon}$) to the applied stress (σ_z) and the test temperature (T).

It is felt from the critical review of the literature that a comprenensive analysis of the creep behaviour of the composite materials is needed.

In this work, a model is developed to describe mathematically the behaviour of composite materials undergoing creep rupture testing. This mathematical model is based mainly on the analysis of the stress field around the fibres, which leads to a proper allocation of stresses to both fibres and matrix.

DEVELOPMENT OF THE MODEL

Under the applied load, the matrix flows and transfers the load to the fibres. The fibre/matrix interaction results in the development of an interfacial shear stress at the fibre/matrix interface (τ_i), which generates a normal stress (σ_{zf}) on the fibres. The balance between these stresses is expressed in the following relation :

$$d\sigma_{zf}/dz = -2\tau_i/r \qquad (2)$$

where (r) is the fibre radius and (z) is the fibre axis.

Fig.1 shows the distribution of (τ_i) , (σ_{zf}) along the fibre length (L). The distribution is symmetrical from the middle of the fibre to either ends, hence, the following description will be confined to (L/2). Along the transfer length (L_c) , (τ_i) is constant and equal to the matrix yield stress (τ_{ym}). This leads to the development of (σ_{zf}) from zero at fibre end to a value (σ_t) at (L_c) with a linear relationship.

Then (τ_i) drops non-linearly to a zero value at (L/2). Correspondingly, (σ_{zf}) increases non-linearly to (σ_{zfmax}).

The thermal residual stress on the fibre (σ_{rf}) resulting from the differential thermal expansion mismatch between fibres and matrix is shown in Fig.1, having a constant value along the fibre length and is obtained from :

$$\sigma_{rf} = E_f.(\alpha_m - \alpha_f).(T_1 - T) \qquad (3)$$

where E_f is the fibre elastic modulus, α_m and α_f are the thermal expansion coefficients for matrix and fibres respectively and (T_1-T) is the temperature difference between the fabrication and the test of the composite.

Fig. 2 illustrates a slab taken in the elastic interaction zone ($0 \leq z < L/2 - L_c$), where the elongation in fibres was (u_f), and in the matrix was varying linearly from (u_f) to (u_m) at the mid-distance between fibres ($\lambda/2$). Balance of forces acting on the slab results in :

$$\tau_m = r.\tau_i/y \qquad (4)$$

where (τ_m) is the shear stress in the matrix at a distance (y) from the fibre axis. Replacing the value of shear modulus (μ_m) of the matrix in equation (4) :

$$du = r.\tau_i/\mu_m.(dy/y) \qquad (5)$$

Integrating equation (5) and differentiating the resulting relation with respect to (z), the following expression can be derived :

$$d\tau_i/dz = E_m.(\epsilon_z - (\sigma_{zf}/E_f))/Cl \qquad (6)$$

where E_m is the matrix elasticity modulus ($\mu_m = E_m/2.(1+\nu_m)$), and Cl is a constant having the value $(r.(1+\nu_m).\ln(\lambda/2r))$. ($\epsilon_z$) is the matrix strain in the z-direction.

Differentiating equation (2) leads to :

$$d^2\sigma_{zf}/dz^2 = -2/r\ .(d\tau_i/dz) \qquad (7)$$

Replacing ($d\tau_i/dz$) from equation (6) into (7) yields :

$$d^2\sigma_{zf}/dz^2 = -2E_m/rCl\ .\ (\epsilon_z - \sigma_{zf}/E_f) \qquad (8)$$

Integrating equation (8) to get (σ_{zf}) will Yield :

$$\sigma_{zf} = 2\,\frac{(\sigma_t - E_f.\epsilon_z)\ .\ \sinh(mL_t)}{\sinh(2m.L_t)}\ .\ \cosh(mz) + E_f\epsilon_z \qquad (9)$$

where $m = (2E_m/E_f.r.Cl)^{0.5}$ and Lt= L/2 -Lc.

Along the transfer length, ($\tau_i = \tau_{ym}$); the following relation exists :

$$\sigma_{zf} = 2\tau_{ym}/r. \quad (L/2 - z) \tag{10}$$

Considering the thermal residual stresses, equations (9) and (10) will have the form :

$$\sigma_{zf} = 2.\frac{(\sigma_t - E_f\epsilon_z).\sinh(mL_t)}{\sinh(2mL_t)}.\cosh(mz) + E_f\epsilon_z + E_f(\alpha_m - \alpha_f).(T_1 - T) \tag{11}$$

$$\sigma_{zf} = 2\tau_{ym}/r. \quad (L/2 - z) \tag{12}$$

It can be easily shown that :

$$\sigma_{zfmax} = \frac{\sigma_t - E_f\epsilon_z}{\cosh(mL_t)} + E_f\epsilon_z + E_f(\alpha_m - \alpha_f).(T_1 - T) \tag{13}$$

Solving equations (11) and (12) as $z = L/2 - L_c$, the value of (L_c) can be determined.

As the stress (σ_{zf}) is determined at any position (z) along the fibre, the corresponding normal stress on the matrix (σ_{zm}) can be obtained from the relation :

$$\sigma_{zm} = (1/(1-V_f)).(\sigma_z - V_f.\sigma_{zf}) \tag{14}$$

Equating the externally applied energy(Ux) to the internal one (Ui), the following will be obtained :

$$Ux = \sigma_z.(e^{\epsilon_z} - 1) \tag{15}$$

$$Ui = \int_{\epsilon_{ym}}^{\epsilon_z} \bar{\sigma}_{zm}\,d\bar{\epsilon}_{zm} + \int_{\epsilon_{yf}}^{\epsilon_z} \bar{\sigma}_{zf}\,d\bar{\epsilon}_{zf} + \sigma_{ym}^2/2E_m + \sigma_{yf}^2/2E_f \tag{16}$$

Equation (16) can be rewritten as :

$$Ui = \int_0^t \bar{\sigma}_{zm}\dot{\epsilon}_m.dt + \int_0^t \bar{\sigma}_{zf}\dot{\epsilon}_f.dt + \sigma_{ym}^2/2E_m + \sigma_{yf}^2/2E_f \tag{17}$$

Replacing equation (1) in equation (17)it yields :

$$Ui = (t.w4/w5).(1+3.C2.(\sigma_{zf}/\sigma_{zm})) + \sigma_{ym}^2/2E_m + \sigma_{yf}^2/2E_f \tag{18}$$

6

where $w4 = A_{2m} D_{ef} b_m \sigma_{zm}^{n+1}$ and $w5 = 9kT(\sqrt{3}\mu_m)^{n-1}$;

C2 is the ratio between the ultimate tensile strain of fibres material to that of the matrix.
A_{2m} is a constant determined by Ashby[1].
b_m is the Burgers vector of the matrix material.
D_{ef} is the effective diffusion coefficient [1].

Equating (Ui) to (Ux), the following is obtained :

$$t = \frac{w5.(\sigma_z(e^{\epsilon_z}-1) - \sigma_{ym}^2/2E_m - \sigma_{yf}^2/2E_f)}{w4.(1 + 3.C2\ (\sigma_{zf}/\sigma_{zm})} \qquad (19)$$

where t is the time to rupture and σ_z is the applied stress on the stress rupture specimens.

APPLICATION OF THE MODEL

The model developed in this work is used to describe the stress rupture behaviour of fibre reinforced composites. Data on the test conditions (stress, σ_z and temperature, T) as well as the material parameters (fibre and matrix elastic modulii E_f, E_m), and structure parameters (fibre radius, r, volume fraction, V_f, and aspect ratio, L/d) constitute the input to a computer program designed to calculate the corresponding time to rupture, t and plot a family of stress rupture curves for the different conditions. A stress concentration factor, C, was introduced to account for microstructural imperfections. Data used are for the Al-Ni insitu composite and the Stainless Steel- Cu, (S.St-Cu), artificial composite. The following is a discussion of the effect of the different variables.

Effect of Test Temperature

The effect of test temperature on the stress rupture of Al-Ni insitu composite and S.St-Cu artificial composite is shown in Figs.3, and 4 respectively. Generally, the curves exhibit a lower level with higher temperature. This is expected in view of the reduction in strength of the composite with increasing temperature. This is reflected in lower E_f, Em and strain hardening exponent. For the same reason the time to rupture decreases with increasing temperature for both composites, as shown in Figs.5, and 6. Increasing temperature also enhances diffusion and leads to higher deformation rates in the composites resulting in lower times to rupture. An additional effect of increasing temperature is the physiochemical stability of the composites microstructure under combined effect of temperature and time. Possible microstructural changes are fibre coarsening and fibre degradation. These instabilities are more pronounced at lower stress levels and longer times and lead to a decrease in the time to rupture of the composites.

Effect of Volume Fraction

Fig.7 shows the effect of volume fraction on the stress rupture curves of S.St-Cu composite. At stresses lower than 330 MPa, the stress rupture curves exhibited a higher level with increasing the volume fraction. This is attributed to the more effective reinforcement associated with increased volume fraction of the reinforcing phase. However, a peculiar behaviour is observed at stresses higher than 330 MPa. The stress rupture curves showed a higher level with lower volume fraction. A direct explanation of this behaviour is not available at the moment. However, this may be physically explained by the increased propability of premature fibre fracture with higher V_f. The effect of volume fraction of the Al-Ni composite was not studied since the input data were only confined to the eutectic composition of Al-6.2%Ni having a constant V_f of 11%.

Effect of Fibre Radius

The effect of fibre radius on the stress rupture curves of Al-Ni composite and S.St-Cu artificial composite are shown in Figs.8 and 9 respectively.The stress rupture curves showed lower levels with increasing fibre radius. Fig.10 also shows the effect of fibre radius of Al-Ni composite on the time to rupture at constant levels of stress. Fig.11 shows the same effect but for the S.St-Cu composite. The time to rupture increases with decreasing fibre radius. The range of fibre radii studied was 0.15-0.4 micron for the insitu composite, while it was 0.2-0.4 mm for the artificial composite.

The above results were expected in view of the well established relationship of enhanced composite strength with increasing fineness of its microstructure. For the same volume fraction, decreased fibre radius means increased fibre/matrix interfacial area and more effective contribution of the reinforcing phase to the total load bearing capacity of the composite. This is accounted for by the model. Moreover, decreased fibre radius results in a lower propability of the existance of fibre imperfections which delays premature fibre fracture, thus increases time to rupture.

Effect of Aspect Ratio

The effect of aspect ratio as a percentage of the critical aspect ratio ($2L_c/d$), on the stress rupture curves of Al-Ni and S.St-Cu composites is shown in Figs. 12,13 respectively. Fig. 14 shows the effect of aspect ratio on the time to rupture at constant stress for both composites. Increasing the aspect ratio leads to a higher level of the stress rupture curves and increased time to rupture for both composites. Increasing aspect ratio enhances the capacity of fibres to withstand high enough normal stresses developed along their length from the interfacial shear stresses acting on the fibre/matrix interface.

6

Higher aspect ratios also helps prematurely broken fibres to be reloaded again. This effectively contributes to the total load bearing capacity of the composite and also delays its failure. The model accurately takes into consideration this effect of aspect ratio of the fibres.

Effect of Microstructural Imperfections

A stress concentration factor, C is introduced into the model to account for the stress concentrations arising from microstructural imperfections. Fig.15,16 show the effect of the stress concentration factor on the stress rupture curves for Al-Ni, and S.St-Cu composites. Fig.17 also shows the effect of factor C on the time to rupture at a constant stress for both composites. It is clearly depicted from the previous figures that increasing C lowers the levels of the stress rupture curves, and decreases the time to rupture for both materials. Microstructural imperfections may lead to premature fibre fracture and the increase of the density of microvoids which will eventually grow and coalesce to form a crack that will propagate and leads to decreased time to rupture.

CONCLUSION

The model developed in this work successfully describes the stress rupture behavior of fibrous composites. The model is based on a micromechanical approach to the interaction between matrix and fibres through the development of interfacial shear stress on the fibre/matrix interface and the corresponding generation of a normal stress on the fibre. The model predict to a reasonable extent, the time to rupture under combined effect of stress and temperature. The model is sensitive to material properties and microstructure parameters. It successfully describes the effect of those parameters on the stress rupture behavior of the composites. The model indicates that increasing fineness and perfection of the microstructure and aspect ratio of the fibres enhances the time to rupture of the composites for the same rupture stress and temperature. However, the model has the limitations that it does not take into consideration the physiochemical instability and it is not applicable for lamellar composites.

REFERENCES

1. Frost,H.J.,"Deformation mechanisms",Pergamon press,1982
2. Piggot,M.R.,"Load-bearing fibre composites",Pergamon,1980
3. Christensen,R.,"Mech. of composite material",McGRAW-HILL
4. Jones,R.M.,"mech. of composite mat.",JOHN WILEY,1975
5. Frost,H.J.,and Ashby,M.F.,Harvard Univ., Final report,1975
6. Benham,P.P.,"Thermal stresses",Pitman &Sons Ltd.,1964
7. Farag,M.M. and Abd El Latif,M.H., Met. Trans.,6A,1316,1973

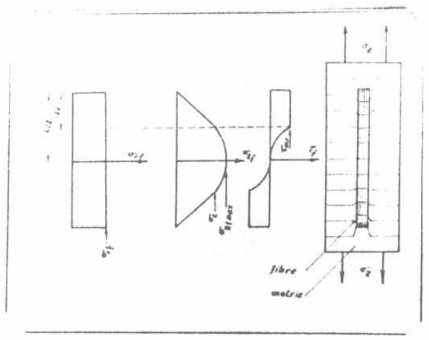

Fig.1. Distribution of interfacial shear stress(τ_i), normal stress(σ_{zf}) and residual stress(σ_{rf}) on fibre length

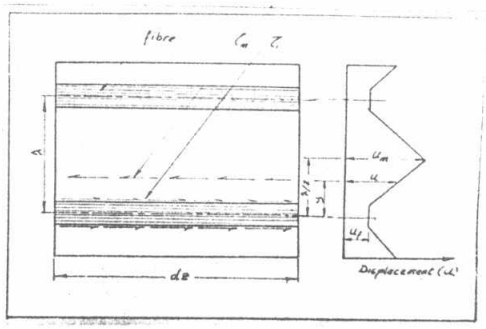

Fig.2. A slab taken in the elastic interaction zone, ($0 < z < (L/2 - L_c)$)

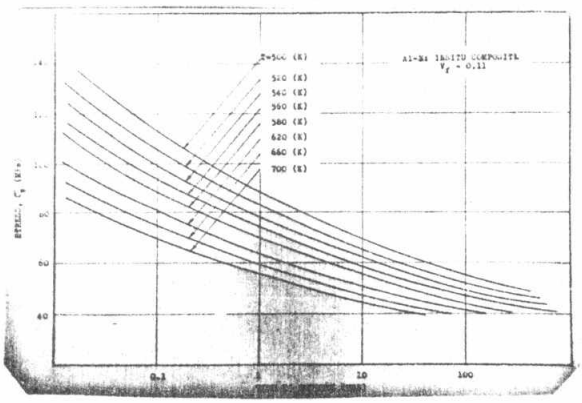

Fig.3. Effect of test temperature on stress rupture curves for Al-Ni composites, reference [7]

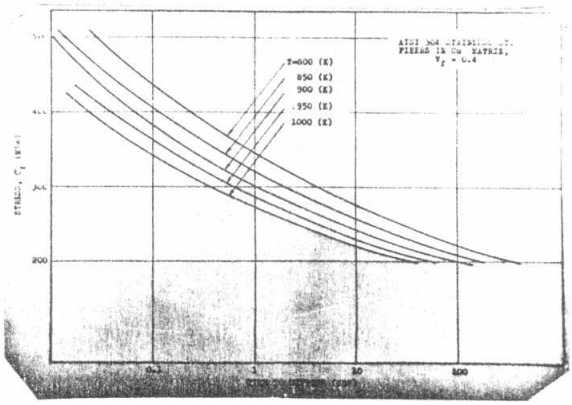

Fig.4. Effect of test temperature on stress rupture curves for S.St-Cu composites

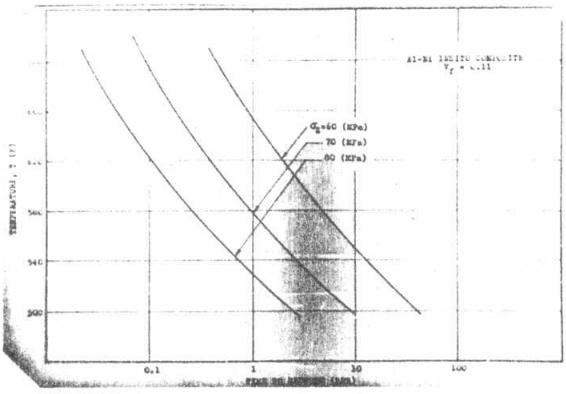

Fig.5. Effect of temperature on time to rupture for Al-Ni composites

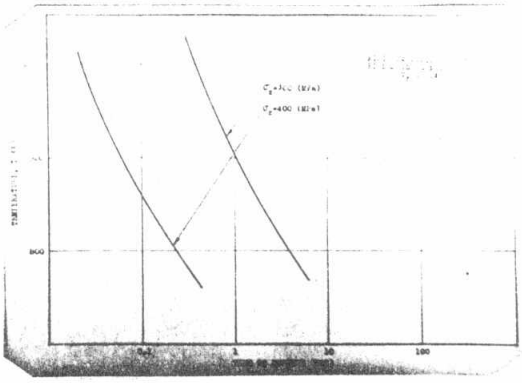

Fig.6. Effect of temperature on time to rupture of S.St-Cu composites

6

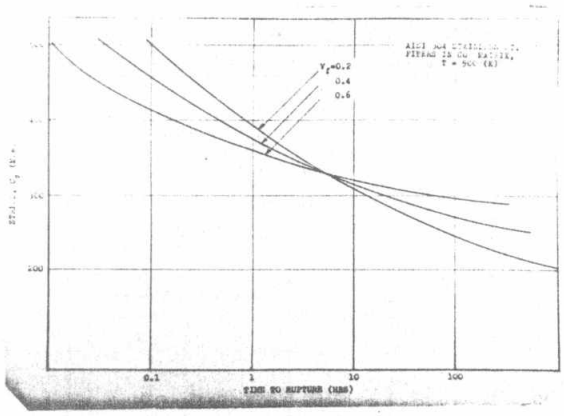

Fig.7. Effect of volume fraction on the stress rupture curves of S.St-Cu composites

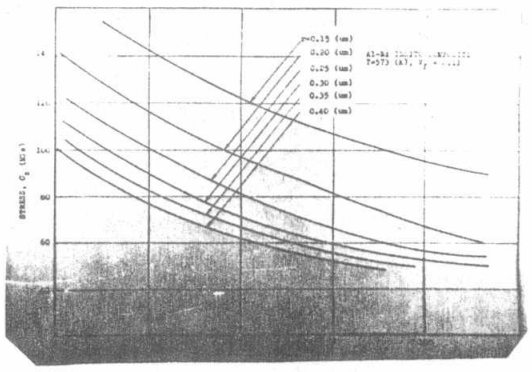

Fig.8. Effect of fibre radius on stress rupture curves of Al-Ni composites

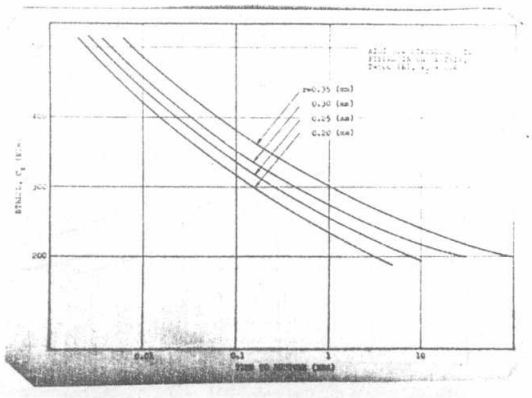

Fig.9. Effect of fibre radius on the stress rupture curves of S.St-Cu composites

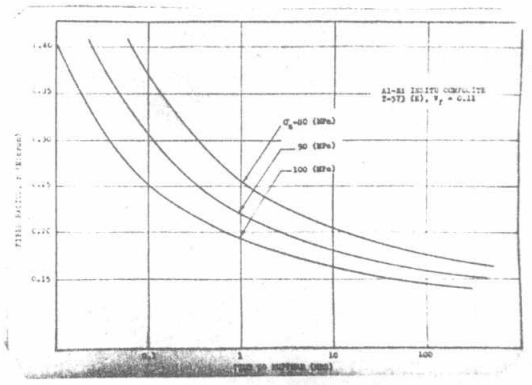

Fig.10. Effect of fibre radius on the time to rupture of Al-Ni composites

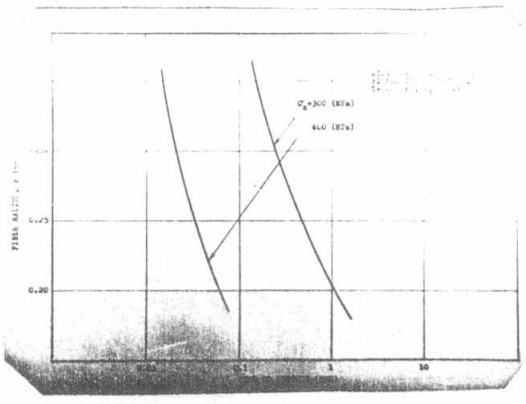

Fig.11. Effect of fibre radius on the time to rupture for S.St-Cu composites

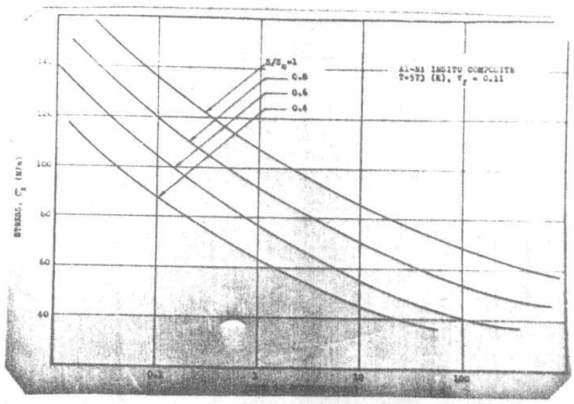

Fig.12. Effect of aspect ratio on the stress rupture curves of Al-Ni composites

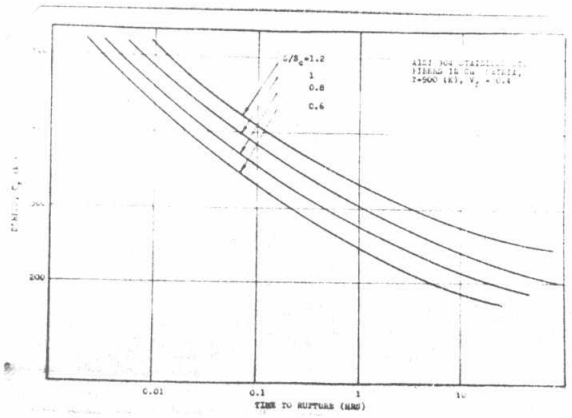

Fig.13. Effect of aspect ratio on the stress rupture curves of S.St-Cu composites

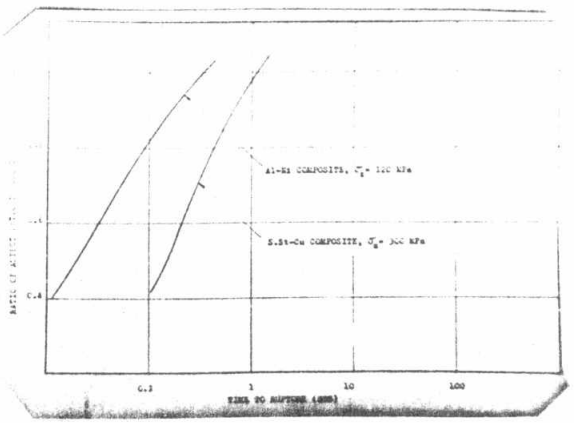

Fig.14. Effect of aspect ratio on time to rupture for both composites

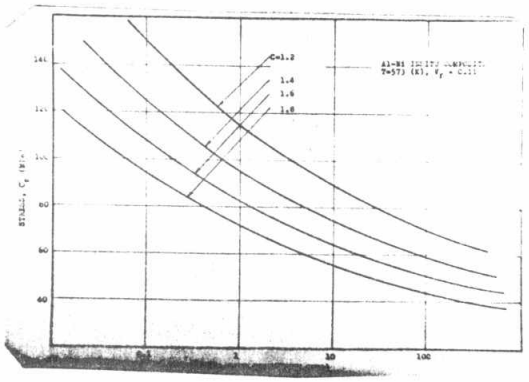

Fig.15. Effect of stress concentration factor on the stress rupture curves of Al-Ni composites

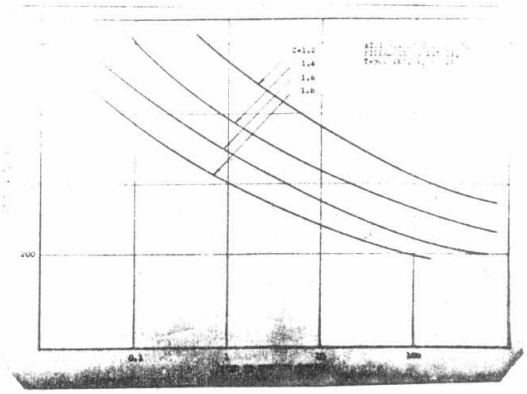

Fig.16. Effect of stress concentration factor on the stress rupture curves of S.St-Cu composites

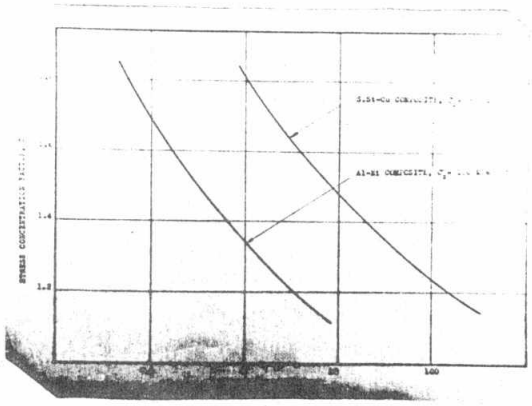

Fig.17. Effect of stress concentration factor on time to rupture for both composites